Mid to late 20th century freshening of the western tropical South Atlantic triggered by southward migration of the Intertropical Convergence Zone

N.S Pereira[1], L.J. Clarke[2], C.M. Chiessi[3], K.H. Kilbourne[4], S. Crivellari[3], F.W. Cruz[5], J.L.P.S. Campos[5], T.-L. Yu[6,7], C.-C. Shen[6,8], R.K.P. Kikuchi[9], B.R. Pinheiro[10], G.O. Longo[11], A.N, Sial[12], T. Felis[13]

[1]*Department of Exact and Earth Sciences, State University of Bahia, Salvador, Brazil.*
[2] *Department of Natural Sciences, Faculty of Science and Engineering, Manchester Metropolitan University, Manchester, UK.*
[3] *School of Arts, Sciences and Humanities, University of São Paulo, São Paulo, Brazil,*
[4] *Chesapeake Biological Laboratory, Maryland University, Solomons, US*
[5] *Institute of Geoscience, University of São Paulo, São Paulo, Brazil*
[6]*HISPEC, Department of Geosciences, National Taiwan University., Taipei, Taiwan, ROC.*
[7]*Marine Industry and Engineer Research Center, National Academy of Marine Research, Koahsiuung, Taiwan, ROC.*
[8]*Research Center for Future Earth, National Taiwan University, Taipei, Taiwan, ROC*
[9]*Department of Oceanography, Federal University of Bahia, Salvador, Brazil.*
[10]*Institute of Biological Sciences and Health, Federal University of Alagoas, Maceió, Brazil.*
[11]*Department of Oceanography and Limnology, Federal University of Rio Grande do Norte, Natal, Brazil*
[12]*NEG-LABISE, Federal University of Pernambuco, Recife, Brazil.*
[13]*MARUM—Center for Marine Environmental Sciences, University of Bremen, Bremen, Germany*

Abstract

In the tropical Atlantic Ocean, the Intertropical Convergence Zone (ITCZ) is an important climate feature controlled by the interhemispheric sea surface temperature (SST) gradient, and greatly influences rainfall patterns over the adjacent continents. To better understand ITCZ dynamics in the context of past and future climate change, long-term oceanic records are needed, but observational data are limited in temporal extent. Shallow-water corals provide seasonally-resolved archives of climate variability over the tropical ocean. Here we present seasonally-resolved records of stable oxygen ($\delta^{18}O$) and carbon ($\delta^{13}C$) isotope values of a *Siderastrea stellata* coral from northeastern Brazil (Maracajaú, ~5°S). We show that the long-term trends in the record of coral $\delta^{18}O$ values are not primarily driven by SST but by hydrological changes at the sea surface. Combining the record of coral $\delta^{18}O$ values with instrumental SST, we present the first reconstruction of seawater $\delta^{18}O$ changes ($\delta^{18}O_{seawater}$) in the western tropical South Atlantic back to the early 20th century, a parameter that is related to changes in sea surface salinity. The reconstructed $\delta^{18}O_{seawater}$ changes indicate a prominent freshening between the mid-1940's and mid-1970's, which coincides with a weakening of the Atlantic interhemispheric SST gradient during this time interval. Our results suggest that the weakened Atlantic SST gradient resulted in a southward shift of the thermal equator that

was accompanied by a southward migration of the ITCZ, resulting in freshening of the western tropical South Atlantic during the mid to late 20th century.

Keywords: *Siderastrea stellata*; Coral archive; Stable oxygen isotopes; Paleoclimatology; ITCZ.

***Corresponding author: Natan S. Pereira e-mail: nspereira@uneb.br**

1. INTRODUCTION

The Intertropical Convergence Zone (ITCZ) is a well-defined zonally-oriented band of high precipitation, centered a few degrees to the north of the equator (Schneider et al. 2014). The ITCZ shows a marked seasonal meridional migration cycle, characterized by a northernmost position attained during boreal fall and a southernmost position during boreal spring (Waliser and Gautier 1993). The ITCZ strongly influences the distribution of rainfall over the tropical Americas, with substantial socio-economic impacts over northeastern Brazil (Nobre and Shukla 1996; Hastenrath 2012).

Observational and modeling studies of the ITCZ indicate that its position is controlled by the meridional sea-surface temperature (SST) gradient, that changes seasonally with solar irradiance, as well as oceanic and atmospheric heat transport (Schneider et al. 2014). However, observational data are extremely limited in temporal extent and many relevant climatic parameters (e.g., precipitation over the ocean) are only available after the start of the satellite era. Ocean salinity records from the Atlantic Ocean, with high enough resolution to resolve the ITCZ, are only available back to the 1970s (Reverdin et al. 2007), although some very sparse data, averaged over large areas of the ocean, are now available for earlier time periods (Friedman et al. 2017). Land-based precipitation records can be longer, but few span the whole 20th century, particularly over South America (e.g. Júnior and Lucena 2020). Thus, high temporal resolution tropical marine paleoclimate records sensitive to ITCZ-related seawater salinity changes are needed to extend our understanding of ITCZ dynamics.

Shallow-water corals can be excellent tropical climate archives (e.g. Weber and Woodhead 1970; Swart 1983; Swart and Grottoli 2003; Felis 2020). They have been used to reconstruct oceanographic and climatic changes in the Caribbean Sea (e.g., von Reumont et al. 2008; Brocas et al. 2016; Fowell et al. 2016), Red Sea (e.g., ; Al-Rousan et al. 2003; Felis and Rimbu 2010; Murty et al. 2018), Pacific Ocean (e.g., Beck et al., 1992; Linsley et al. 2010; Carilli et al. 2014) and Indian Ocean (e.g., Gagan et al. 1996; Lee et al. 2014). Those studies shed light on ocean–climate system phenomena like the equatorial monsoon (Gagan et al. 1994; Charles et al. 1997; Klein et al. 1997), El Niño Southern Oscillation (ENSO) (e.g. Fairbanks et al. 1997; Hereid et al. 2012; Cobb et al. 2013; Hetzinger et al. 2016) and the ITCZ (Saenger et al. 2008).

In contrast, only a few shallow-water coral records have been generated from corals sampled in the western tropical South Atlantic (Table 1) (Evangelista et al. 2007, 2018; Mayal et al. 2009; Pereira et al. 2016, 2017, 2018). These studies exclusively explored two sites (i.e., Rocas atoll and Abrolhos) from all available Brazilian reef systems (Leão et al. 2016). The few existing coral records from the western tropical South Atlantic provide valuable information, but do not extend long enough back in time to facilitate a full understanding of the influence of climate modes and solar forcing in this understudied region. Among the species with high potential for past climate reconstruction, the coral species *Siderastrea stellata* is one of the most important Brazilian reef builders, with a spatial distribution ranging from the equator to 23°S (Lins-de-Barros and Pires 2007). Furthermore, this coral species may provide geochemical records up to 300 years or more in duration, substantially extending instrumental climate records from the western tropical South Atlantic.

98 **Table 1. Coral-based paleoclimate records from the western tropical South Atlantic,**
99 **covered period and used paleoclimate proxy.**

Species	Location	Period	Proxy	Reference
Mussismilia braziliensis	Abrolhos reefs	1987 -2003	Sr/Ca, Ba/Ca, Mg/Ca	(Santedicola et al. 2008)
Mussismilia braziliensis	Abrolhos and Tinharé Reef	1998-2005	Growth rate	(Kikuchi et al. 2013)
Siderastrea stellata	Abrolhos	1883-2005	Growth rate	(Evangelista et al. 2015)
Porites astreoides	Rocas atoll	2002-2012	$\delta^{18}O$, $\delta^{13}C$	(Pereira et al. 2015)
Mussismilia leptophylla	Abrolhos	1939–1977	Growth rate	(Evangelista et al. 2007)
Siderastrea stellata, *Porites astreoides* and *Montastrea cavernosa*	Rocas atoll	-	$\delta^{53}Cr$, $^{87}Sr/^{86}Sr$, $\delta^{13}C$	(Pereira et al. 2016)
Porites astreoides	Rocas atoll	2001-2013	$\delta^{18}O$, $\delta^{13}C$, Sr/Ca	(Pereira et al. 2017)
Siderastrea stellata	Rocas atoll	1948-2013	$\delta^{13}C$	(Pereira et al. 2018)
Siderastrea stellata	Rocas atoll	1970-2009	Sr/Ca, U/Ca	(Evangelista et al. 2018)
Mussismilia hispida	Rocas atoll	1943-1962	$\delta^{18}O$, $\delta^{13}C$	(Silva et al. 2019)
Siderastrea stellata	Maracajaú Reef	1927-2018	$\delta^{18}O$, $\delta^{13}C$	This study

100

101 Here we present records of stable oxygen ($\delta^{18}O$) and carbon ($\delta^{13}C$) isotope values
102 for a first *Siderastrea Stellata* coral sampled from the Maracajaú reef, situated off
103 northeastern Brazil, covering the period from 1929 to 2018. These coral-based stable
104 isotope records are by far the longest (i.e., 90-years duration) and highest resolved (i.e.,
105 ca. 8 data points per year) datasets from the western tropical South Atlantic. Previous
106 work has reported a relatively low performance of the Sr/Ca-temperature proxy in
107 tracking SST at interannual and longer timescales off Brazil, when applied to a
108 *Siderastrea stellata* coral from Rocas Atoll (Evangelista et al. 2018). Consequently, we
109 pair coral $\delta^{18}O$ with available instrumental seawater temperatures, in order to provide
110 the first reconstruction of the oxygen-isotope composition of seawater ($\delta^{18}O_{seawater}$) and
111 assess changes in sea surface salinity (SSS), and ITCZ position, in the western tropical

South Atlantic throughout the 20th Century. We note that application of the Sr/Ca-temperature proxy to tropical North Atlantic corals of the same genus, *Siderastrea sideria*, has provided more promising results in terms of tracking long-term SST variability (Maupin 2008; DeLong 2014, 2016; Kuffner 2017; Weerabaddana 2021).

2. STUDY AREA

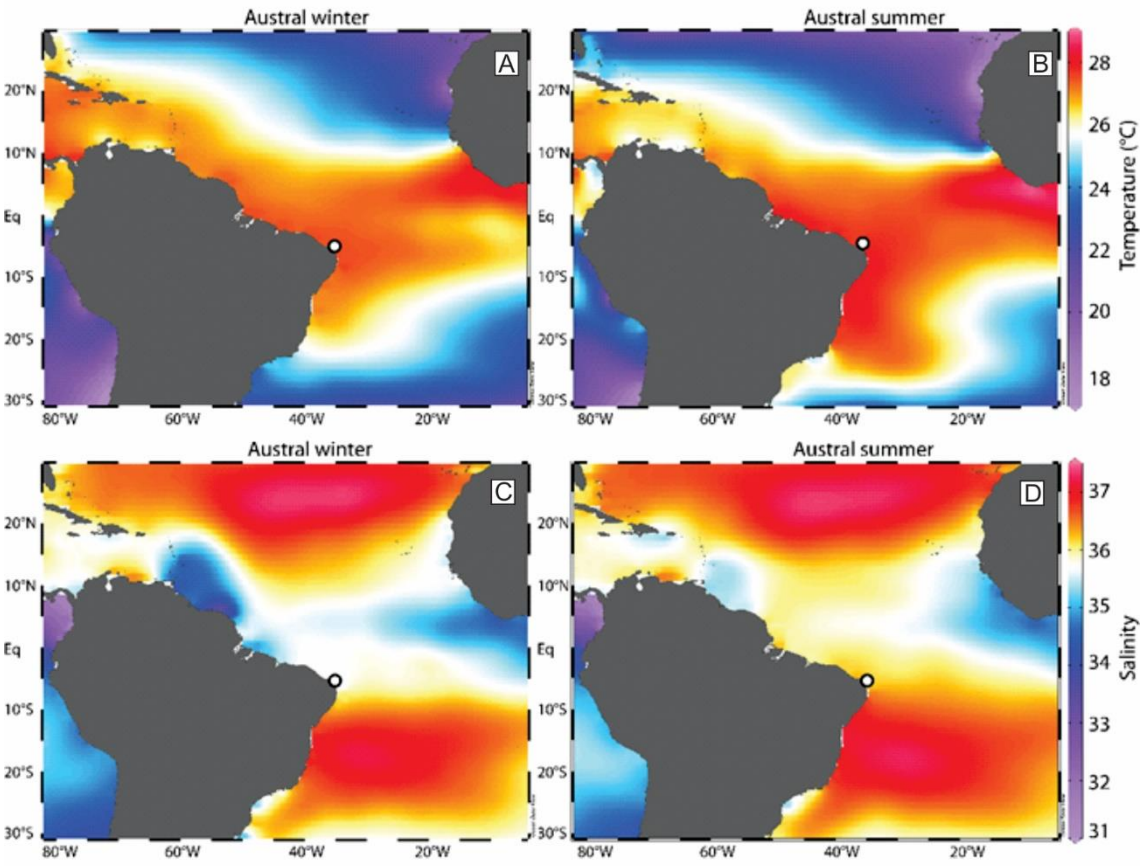

Figure 1. Sea-surface temperature (A and B) and sea-surface salinity (C and D) of the western tropical South Atlantic during austral winter (June-July-August) (A and C) and summer (December-January-February) (B and D). *Siderastrea stellata* coral sampling location at Maracajaú reef is represented by a white circle.

This study presents new records of stable carbon and oxygen isotope values for a *Siderastrea stellata* coral core collected from the shallow coastal reefs of Maracajaú, these spanning from approximately 5º21'12'' S to 5º25'30'' S and from 35º 14' 30'' W to 35º17'12'' W, off northeastern Brazil (Fig. 1).

The regional climate is tropical, with warm humid conditions and a well-defined dry season from September to February, contrasting with a wet season from April to August, with peak precipitation during March–April, when the ITCZ is situated over northern northeastern Brazil (Chiessi et al. 2021). Wind speed peaks during the wet season, when SST reaches 26.5°C, and is weaker during the dry season, when seawater temperature reaches maxima of up to 29.0°C (Testa and Bosence 1999).

The Maracajaú reefs are part of an extensive reef complex (~30 km in length from North to South), situated 5–7 km from the coastline and forming knolls and patch reefs trending in a northwest–southeast direction, parallel to the coast (Santos et al., 2007). The study location is situated within the largest coral patch within the Maracajaú reef complex, this being about 9 km in length and 3 km in width. Water depths in the complex range from a maximum water depth ca. 5 m to partially exposed patches during the lowest tides. Scleractinian corals comprise the reef structure, with *S. stellata* responsible for about 80% of reef construction, alongside calcareous algae (Laborel 1970). The Maracajaú reefs do harbor other scleractinian corals, such as *Porites astreoides, Favia gravida, Agaricia fragilis Agaricia agaricites, Porites branneri, Meandrina braziliensis, Mussismilia hartii* (Santos et al., 2007) and *Mussismilia hispida* (rare, Roos et al. 2019), as well as the hydrocorals *Millepora alcicornis,* which form crowns on the reef tops, and less abundant *Millepora braziliensis* (Santos et al., 2007).

3. MATERIAL AND METHODS

3.1. Sea Surface Temperature

We used SST data from HadISST (Rayner et al. 2003) over the grid point 7º 30’ 00’’ S and 32º 30’ 00’’ W, available at the KNMI Climate Explorer (https://climexp.knmi.nl). To evaluate possible differences between different SST data

products, we also assessed the ERSSTv5 reanalysis data product (Huang et al. 2017), and the high-resolution satellite Oiv2 SST data products (Reynolds et al. 2002), obtained from the same coordinates (see supplementary information**)**. The high correlation between the SST data products indicates that there is no significant difference between them (Fig. S1) and we decide to use the HadISST data product for the further analyses developed in this work.

3.2. Coral sampling

A core of the coral species *Siderastrea stellata* (sample identification number 18SM-C2) was collected from the Maracajaú reef from a water depth ca. 1 m using a pneumatic drill, retrieving a 34 cm long core. Core 18SM-C2 then was cut into two halves, with one half cut into 5 mm thick slices, parallel to the growth axis of the whole *S. stellata* colony. After cutting, the coral slices were cleaned with deionized water, air-dried and then X-rayed at 50 kV and 320 mA, with an exposure time of 3.2 s and a distance from equipment to the object of 108 cm.

A total of 870 carbonate powder samples were collected by continuous, progressive milling to 1 mm depth (using a Proxxon micro mill MF 70 coupled with a precision X-Y table) of the coral slab from the top towards the bottom of the colony, following the thecal wall, with samples taken in 0.4 mm intervals along the growth axis. This sampling resolution resulted in about 8 samples per year (using the mean growth rate as a reference).

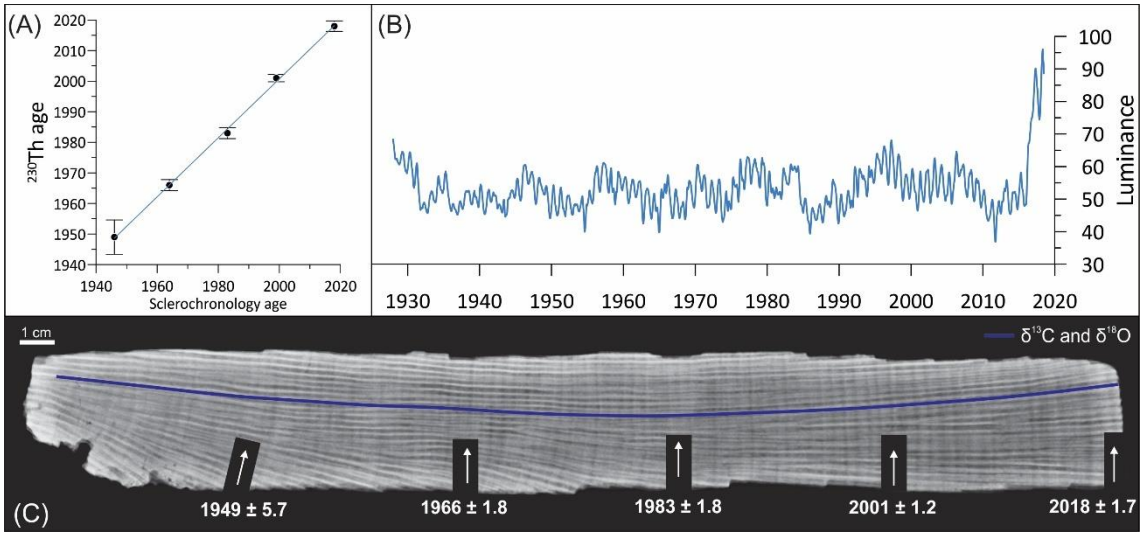

Figure 2. (A) ^{230}Th ages versus sclerochronology ages (r^2 = 0.99, p < 0.0001). (B) Sclerochronology results from CoralXDS analysis. (C) Coral core 18SM-C2 X-ray image with sampling track for stable carbon and oxygen isotope analyses (blue line), as well as sampling locations for ^{230}Th dating (white arrows).

3.3. Geochemical analyses

3.3.1. ^{230}Th dating

Six 0.10–0.25 g subsamples were cut out from along the coral growth axis (Fig. 2) for high precision ^{230}Th dating (Shen et al. 2008, 2012). These subsamples were gently crushed, physically cleaned with ultrasonic methods, and dried for U-Th chemistry. Chemistry was conducted in a class-10,000 metal-free clean room with class-100 benches at the High-Precision Mass Spectrometry and Environment Change Laboratory (HISPEC), Geosciences Department, National Taiwan University (Shen et al., 2008). U–Th isotopic compositions and concentrations were determined on a multi-collector inductively-coupled plasma mass spectrometer (MC-ICP-MS) in the HISPEC (Shen et al., 2012). The half-lives of U–Th nuclides used for ^{230}Th age calculation are the given half-lives reported in Cheng et al. (2013). Uncertainties in the U–Th isotopic data and ^{230}Th dates are calculated at the 2σ level (two standard deviations of the mean, $2\sigma_m$), unless otherwise noted.

194 *3.3.2. Stable-isotope ratio records*

195 Values of $\delta^{13}C$ and $\delta^{18}O$ of 870 milled coral powder samples were determined at
196 the Paleoceanography and Paleoclimatology Laboratory, School of Arts, Sciences and
197 Humanities, University of São Paulo, using a Thermo Scientific™ MAT253 isotope ratio
198 mass spectrometer coupled to a Thermo Scientific™ Kiel IV automated carbonate
199 preparation device. Stable isotope measurements were obtained by reaction of 35–100
200 mg of aragonite with 102% phosphoric acid at 70 °C and the results corrected to permil
201 units relative to Vienna Pee Dee Belemnite (VPDB) using a calcite-based correction (Kim
202 et al., 2007). The SHP2L Solnhofen limestone was used as an internal working standard,
203 which has been calibrated against Vienna Pee Dee Belemnite (VPDB) using the NBS19
204 standard (Crivellari et al. 2021). Analytical precision was better than ±0.05 ‰ for $\delta^{13}C$
205 and ±0.07 ‰ for $\delta^{18}O$ ($\pm 1\ \sigma$, $n = 141$).

206

207 **3.4. Coral core chronology**

208 An age model was developed by counting the density bands using the software
209 CoralXDS (Helmle et al. 2002) and contrasted to radiometric ^{230}Th dating (Fig. 2). Then
210 we compared these results with the number of $\delta^{18}O$ cycles, assuming that the consecutive
211 minima or maxima represent a single year and converted geochemical records from depth
212 in the coral core to a timescale by pairing highest (and lowest) $\delta^{18}O$ with minimum (and
213 maximum) HadiSST data for the region using the software QanalySeries (Kotov and
214 Pälike 2018).

215 **3.5. Seawater $\delta^{18}O$ reconstruction**

216 Values of $\delta^{18}O_{seawater}$ were deconvoluted from paired coral $\delta^{18}O$ and instrumental
217 SST (HadISST), by adjusting the equation proposed by Cahyarini et al. (2008). To
218 remove the SST signal from the coral $\delta^{18}O$ record and retrieve the $\delta^{18}O_{seawater}$ signal we

subtracted the SST contribution, inferred by centered SST, from the centered coral $\delta^{18}O$ signal, according to Equation 1 (for more details see Cahyarini et al. 2008 and Pfeiffer et al. 2019):

Eq (1) $$\delta^{18}O_{seawater} = \left(\delta^{18}O_{coral} - \overline{\delta^{18}O_{coral}}\right) - (\gamma 1) * (SST - \overline{SST})$$

where $\delta^{18}O_{coral}$ is the measured coral sample, $\overline{\delta^{18}O_{coral}}$ is the mean value of measured $\delta^{18}O_{coral}$ samples, SST is the monthly value obtained from HadISST and equivalent in time to the $\delta^{18}O_{coral}$ measured on coral, $\overline{SST}$ is the mean value of SST over the period studied. Γ_1 is the regression slope of $\delta^{18}O_{coral}$ versus SST retrieved from HadISST.

The correlation between $\delta^{18}O_{coral}$ and SST (Fig. 3) yields a $\delta^{18}O_{coral}$–SST relationship of −0.17‰ per 1°C ($r = -0.55$, $p < 0.0001$), a value slightly higher than the slope of −0.138 ‰ per 1°C reported by Maupin et al. (2008) for *Siderastrea siderea* in the Atlantic Ocean, although those authors argue that their slope was likely flatter than it should have been because of their positive SSS (*i.e.* seawater $\delta^{18}O$ contribution) and SST relationship, which dampens the $\delta^{18}O_{coral}$–SST relationship. Although the calibration slope for the Maracajaú *S. stellata* coral is very similar to the well-known slopes for $\delta^{18}O_{coral}$–SST in the Indo-Pacific *Porites* corals (e.g., (Gagan et al., 1998; Omata et al., 2006), the region of Maracajaú is marked by the co-variation of $\delta^{18}O_{seawater}$ and SST, thus the slope obtained by the linear regression between SST and $\delta^{18}O$ might be biased (Cahyarini et al. 2008). In order to evaluate a possible bias, we tested the influence of different linear regression slopes on the reconstructed $\delta^{18}O_{seawater}$. Therefore we compared the $\delta^{18}O_{seawater}$ values obtained based on our linear regression (−0.17‰ per 1°C) to the values obtained based on the linear regressions from Maupin et al. (2008) (−0.138‰ per 1°C) and Juillet-Leclerc and Schmidt (2001) (−0.20‰ per 1°C) (see supplementary material). We found no substantial difference on the long-term trend of the reconstructed

$\delta^{18}O_{seawater}$ when the three different slopes were applied. However, we prefer to use the linear regression slope value from the work of Juillet-Leclerc and Schmidt (2001) avoiding further issues concerning the influence of seawater isotopic composition on the $\delta^{18}O_{coral}$ record and a possible bias generated by the covariation of SST and $\delta^{18}O_{seawater}$.

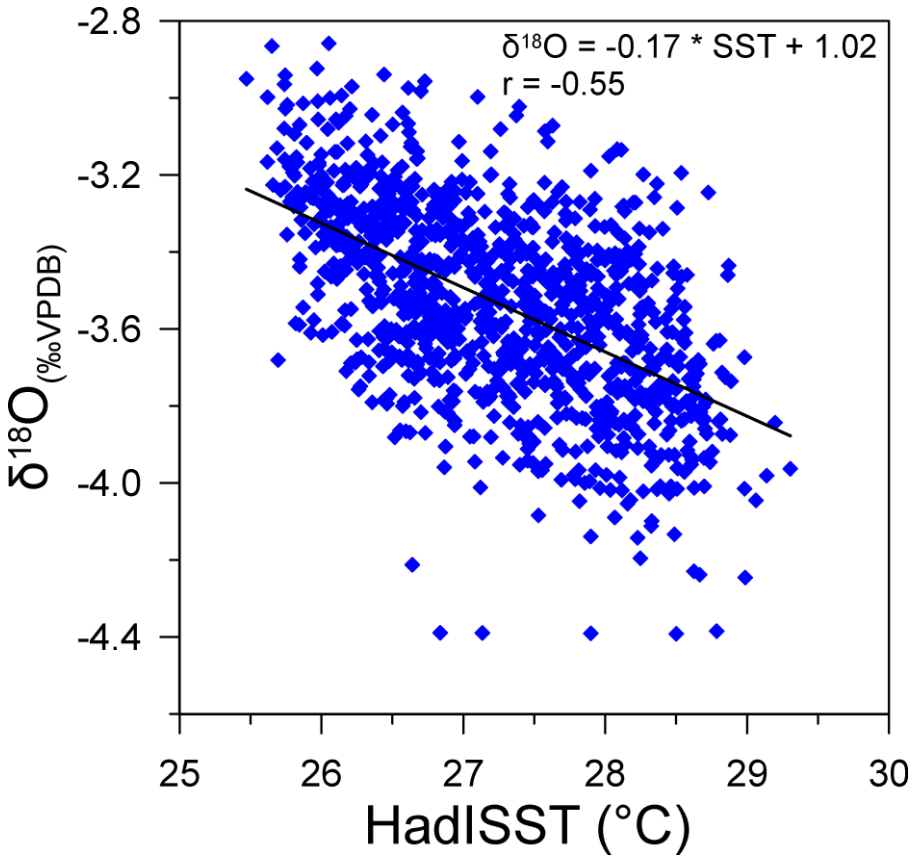

Figure 3. $\delta^{18}O$–SST correlation for coral 18SM-C2 and HadISST (for grid point −7.5 (latitude) and −32.5 (longitude)). The linear regression of $\delta^{18}O$–SST is significant (r = −0.55 p < 0.0001) and the slope is −0.17‰ per 1°C (95% CI: −0.19, −0.15).

3.5.1. Error propagation

The propagated error of reconstructed $\delta^{18}O_{seawater}$ was determined using equation (2), modeled after Cahyarini et al., 2008, where $\sigma_{\delta sw}$ is the error on reconstructed $\delta^{18}O_{seawater}$, $\sigma_{\delta c}$ is the error on measured $\delta^{18}O_{coral}$, γ_1 is the regression slope of $\delta^{18}O_{coral}$ versus SST retrieved from HadISST and σ_{SST} is the error of the HadISST.

Eq (2) $$\sigma_{\delta sw}^2 = \sigma_{\delta c}^2 + (\gamma_1)^2 \sigma_{SST}^2$$

Combining the analytical error of ±0.07‰ for coral $\delta^{18}O$ and HadISST error varying from 0.10 to 0.76 °C, and the slope value for the $\delta^{18}O_{coral}$–SST relationship (γ_1) of −0.17‰ per 1°C, resulted in an error varying from 0.07 to 0.147 ‰ (Figure 6C), with a mean error of ±0.085‰ (1σ) for $\delta^{18}O_{seawater}$.

4. RESULTS AND DISCUSSION

4.1. Age model and *S. stellata* coral growth rates

Density-band counting revealed that coral core 18SM-C2 spans the interval from 1928 to 2018. U-Th isotopic compositions and ^{230}Th dates determined for this coral are listed in Table 2 and the geochronological approach agrees with density-band counting (Fig. 2).

Excluding the first (1928) and last (2018) years, which might not represent a complete year of coral growth, the Maracajaú reef *S. stellata* growth rate varied from 2.1 to 5.8 mm year^{-1}, with a mean growth rate of 3.8 ± 0.7 mm year^{-1} (Fig. 2). The lowest growth rates were during 1987 (2.1 mm year^{-1}), 1937 and 1962 (2.5 mm year^{-1}), 1961 (2.5 mm year^{-1}), 1938, 1941 and 1986 (2.7 mm year^{-1}). The highest growth rates were during 2012 (5.2 mm year^{-1}), 1993 (5.2 mm year^{-1}), 1955 (5.4 mm year^{-1}), 1959 (5.5 mm year^{-1}) and 1944 (5.8 mm year^{-1}).

278 Table 2. U-Th isotopic compositions and ^{230}Th ages for subsamples of coral core 18SM-C2.

Sample ID	Weight g	^{238}U $10^{-6}g/g$ [a]	^{232}Th $10^{-12}g/g$	$\delta^{234}U$ measured[a]	$[^{230}Th/^{238}U]$ activity[c]	$^{230}Th/^{232}Th$ atomic (x 10^{-6})	Age (yr ago) uncorrected	Age (yr ago) corrected [c,d]	Age (yr BP) relative to 1950 AD	$\delta^{234}U_{initial}$ corrected[b]
18SD-1	0.2013	**2.3016 ± 0.0020**	**325.6 ± 2.5**	**146.0 ± 1.4**	**0.0000421 ± 0.0000045**	**4.90 ± 0.53**	**4.00 ± 0.43**	**0.7 ± 1.7**	**-68.8 ± 1.7**	**146.02 ± 1.4**
18SD-2	0.2122	**2.3994 ± 0.0023**	**225.6 ± 2.2**	**145.4 ± 1.5**	**0.0002094 ± 0.0000046**	**36.71 ± 0.89**	**19.93 ± 0.44**	**17.8 ± 1.2**	**-51.8 ± 1.2**	**145.39 ± 1.5**
18SD-3	0.2025	**2.0174 ± 0.0017**	**286.7 ± 2.3**	**143.0 ± 1.3**	**0.0004106 ± 0.0000069**	**47.64 ± 0.89**	**39.18 ± 0.66**	**35.9 ± 1.8**	**-33.8 ± 1.8**	**143.03 ± 1.3**
18SD-4	0.2024	**2.2394 ± 0.0019**	**311.8 ± 2.4**	**144.0 ± 1.3**	**0.0005929 ± 0.0000079**	**70.2 ± 1.1**	**56.53 ± 0.76**	**53.3 ± 1.8**	**-16.2 ± 1.8**	**144.03 ± 1.3**
18SD-5	0.2440	**2.3284 ± 0.0028**	**1113.6 ± 2.4**	**142.1 ± 1.5**	**0.000849 ± 0.000015**	**29.25 ± 0.53**	**81.0 ± 1.5**	**70.0 ± 5.7**	**0.23 ± 5.7**	**142.17 ± 1.5**

Analytical errors are 2σ of the mean.

[a] $[^{238}U] = [^{235}U] \times 137.77$ (±0.11‰) (Hiess et al., 2012); $\delta^{234}U = ([^{234}U/^{238}U]_{activity} - 1) \times 1000$.

[b] $\delta^{234}U_{initial}$ corrected was calculated based on ^{230}Th age (T), i.e., $\delta^{234}U_{initial} = \delta^{234}U_{measured} X e^{\lambda 234 * T}$, and T is corrected age.

[c] $[^{230}Th/^{238}U]_{activity} = 1 - e^{-\lambda_{230}T} + (\delta^{234}U_{measured}/1000)[\lambda_{230}/(\lambda_{230} - \lambda_{234})](1 - e^{-(\lambda_{230} - \lambda_{234})T})$, where T is the age.

Decay constants are 9.1705×10^{-6} yr^{-1} for ^{230}Th, 2.8221×10^{-6} yr^{-1} for ^{234}U (Cheng et al., 2013), and 1.55125×10^{-10} yr^{-1} for ^{238}U (Jaffey et al., 1971).

[d] Age corrections, relative to chemistry date on July 15th and September 26th, 2019, were calculated using an estimated atomic $^{230}Th/^{232}Th$ ratio of 4 (± 2) x 10^{-6} (Shen et al., 2008).

279

280

Before interpretations of the records of $\delta^{18}O$ and $\delta^{13}C$ values can be made, it is important to assess possible growth-rate related kinetic effects (McConnaughey 1989; Cohen and McConnaughey 2003), which could compromise coral geochemistry-based reconstructions of SST, and ultimately SSS. For the coral *S. stellata* from Maracajaú reef, there was no statistically significant relationship between annual growth rates and annual mean $\delta^{18}O$ and $\delta^{13}C$ values ($p>0.05$; Fig. 4). Consequently, coral core 18SM-C2 $\delta^{18}O_{coral}$ variability seems to be independent of growth rate related kinetic effects (McConnaughey 1989; Cohen and McConnaughey 2003).

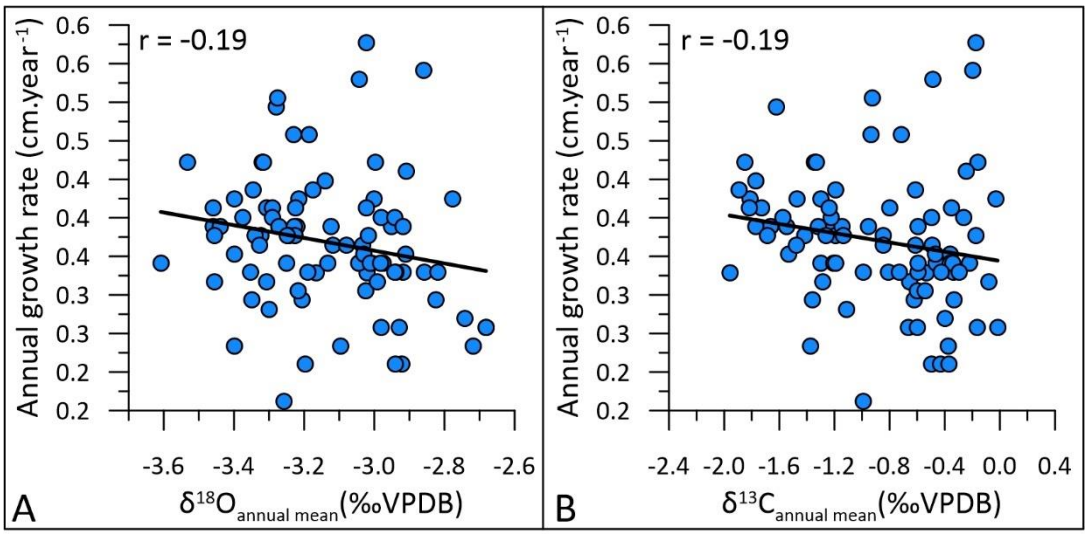

Figure 4. Comparison between Maracajaú reef *S. stellata* coral colony 18SM-C2 annual growth rate and mean annual $\delta^{18}O$ ($p = 0.06$) (A); and $\delta^{13}C$ ($p = 0.08$) (B) values.

4.2. *S. stellata* $\delta^{13}C$ record

Data records of HadISST SST and Maracajaú reef *S. stellata* $\delta^{13}C$ and $\delta^{18}O$ records and growth rate are shown in Figure 5.

S. stellata $\delta^{13}C_{coral}$ values (Fig.5) vary from −2.64 to 0.44‰ and the $\delta^{13}C_{coral}$ record exhibits short-term (i.e., seasonal or intra-annual) variations, which are usually interpreted as a result of seasonal changes in cloud cover and the availability of light. Light availability influences coral zooxanthellae symbiont uptake of ^{12}C, seasonally

changing the carbon-isotope composition of the internal dissolved inorganic carbon pool, from which the coral skeleton is precipitated (Fairbanks and Dodge 1979; Pätzold 1984; Grottoli and Wellington 1999). The $\delta^{13}C_{coral}$ record also shows a general long-term trend to lower values, after the 1940s. This pattern is consistent with the Suess Effect (Revelle and Suess 1957; Keeling 1979) which describes the release of ^{13}C-depleted CO_2 into the atmosphere via the burning of fossil fuels, and the subsequent dissolution of such CO_2 into the oceans. Similar $\delta^{13}C_{coral}$ trends have been observed in corals from other Atlantic Ocean sites (Swart et al. 2010) and the Maracajaú reef *S. stellata* decreasing trend of −0.019‰ per year is consistent with those values reported by Pereira et al. (2018b) for other Brazilian *Siderastrea* corals sampled from 1948 and 2013 (Table 1).

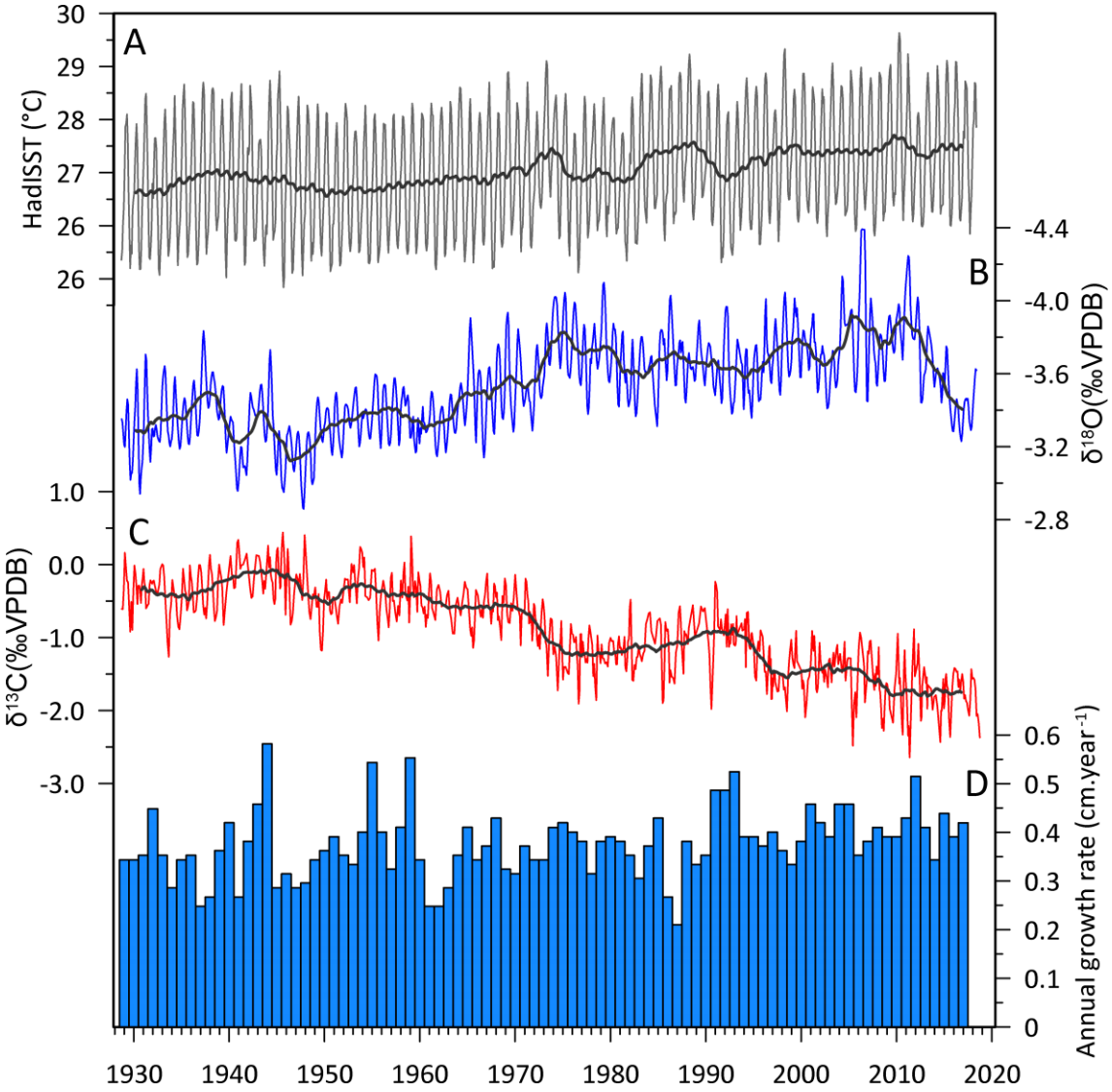

Figure 5. A) Sea surface temperatures (SST) for the Maracajaú reef obtained from the HadISST product (Kennedy et al. 2019) retrieved from https://climexp.knmi.nl for the grid point −7.5 (latitude) and −32.5 (longitude). Maracajaú reef *S. stellata* coral core 18SM-C2 $\delta^{18}O$ and $\delta^{13}C$ time series (B and C, respectively). (D) Coral core 18SM-C2 annual growth rate. Thick black lines in A-C are running (37-point window) averages.

4.3. *S. stellata* $\delta^{18}O$ record

Gridded instrumental SST for the Maracajaú reef region varied from 25.47 to 29.30°C, with a mean of 27.26 ± 0.84°C and maximum range of 3.83°C, for the period from 1928 to 2018 (Fig. 5). The SST time series exhibits an overall general increasing trend of 0.007°C per year, corresponding to an SST increase of 0.63°C through the 90-year study interval.

S. stellata $\delta^{18}O_{coral}$ varied from −4.00 to −2.43‰; the $\delta^{18}O_{coral}$ record shows clear lower magnitude seasonal (intra-annual) cycles contrasting with larger magnitude interannual variability. The complete Maracajaú reef *S. stellata* $\delta^{18}O$ record does not correlate strongly with the independent HadISST SST record for the study region; only 30% of $\delta^{18}O$ variance is explained by SST ($r^2 = 0.30$, $p<0.001$), such that 70% of the $\delta^{18}O$ variance must be explained by other forcing variables. Since *S. stellata* growth rate does not exhibit any strong correlation with $\delta^{18}O$ ($r^2 = 0.04$, $p = 0.06$), the next most plausible explanation is that $\delta^{18}O_{coral}$ variability has been influenced by changing surface seawater salinity (SSS). Nevertheless, it is important to recognize that, under specific conditions (e.g. enclosed reef pools), $\delta^{18}O_{coral}$ records may be better recorders of more localized, reef-scale, SST conditions (Huang et al. 2017; Pfeiffer et al. 2019) than available wider-scale SST datasets retrieved from combined satellite and in-situ measurements, the latter also often comprising scarce data measurements that have been averaged across large spatial scales.

An important feature within the $\delta^{18}O_{coral}$ record is an overall decreasing trend, to lower $\delta^{18}O$ values, from the mid-1940s and to the mid-1970s, that is decoupled from the long-term variability evident in the HadISST SST record. Over this time interval, $\delta^{18}O_{coral}$ has an overall decreasing trend of −0.0056‰ per year, with a total decrease of −0.50‰. Conversion of $\delta^{18}O_{coral}$ into SST (assuming the $\delta^{18}O$-SST relationship of 0.17‰/°C), produces a trend with an annual SST increase of 0.033°C and a total rise of 2.96°C for this time interval, more than 4 times the HadISST SST increase for the region. Even when assuming a 'traditional' $\delta^{18}O$-SST relationship of 0.22‰/˚C slope (Juillet-Leclerc and Schmidt 2001), the observed −0.50‰ decrease in $\delta^{18}O_{coral}$ represents more than 2˚C increase in SST, indicating that the identified long-term $\delta^{18}O_{coral}$ trend must be influenced by another factor, the most likely one being a change in $\delta^{18}O_{seawater}$. Possible causes of

which include the addition of freshwater into the marine system and/or decreased evaporation from the ocean surface.

As detailed above, the largest magnitude Maracajaú reef *S. stellata* $\delta^{18}O_{coral}$ decreasing trend occurs from the mid-1940s to the mid-1970s (Fig. 4), with a subsequent lower magnitude general decrease between the mid-1970s and ca. 2010. The change in coral $\delta^{18}O$ from 1945 to 1975 is -0.55‰, whereas the change in SST over the same period is +0.09˚C. Thus, the SST trend can only explain a small fraction of the $\delta^{18}O$ change. We suggest that the decreasing trend in coral $\delta^{18}O$ from 1945 to 1975 was caused by a freshening in the upper western tropical South Atlantic.

4.4. $\delta^{18}O_{seawater}$ reconstruction

Decoupling the HadISST SST signal from the Maracajaú reef *S. stellata* $\delta^{18}O_{coral}$ record (section 3.3.1) results in a $\delta^{18}O_{seawater}$ reconstruction with a total range of 1.20‰ across the study time interval (Fig. 6). One of the main features of this $\delta^{18}O_{seawater}$ reconstruction is an overall decreasing trend, to more negative $\delta^{18}O$ values, from ca. 1947 to ca. 1975. Prior to 1947, average $\delta^{18}O_{seawater}$ values were 0.17 ± 0.15‰ and between 1975 and ca. 2012 average $\delta^{18}O_{seawater}$ values were −0.16 ± 0.16‰; both time intervals also exhibit some variability in reconstructed $\delta^{18}O_{seawater}$. After the 1980s, the $\delta^{18}O_{seawater}$ trend stabilized with substantial interannual variations, from ca. 2012, reconstructed $\delta^{18}O_{seawater}$ increases in magnitude, to more positive values, coincident with the most intense drought in northeastern Brazil in recent decades (Brito et al. 2018).

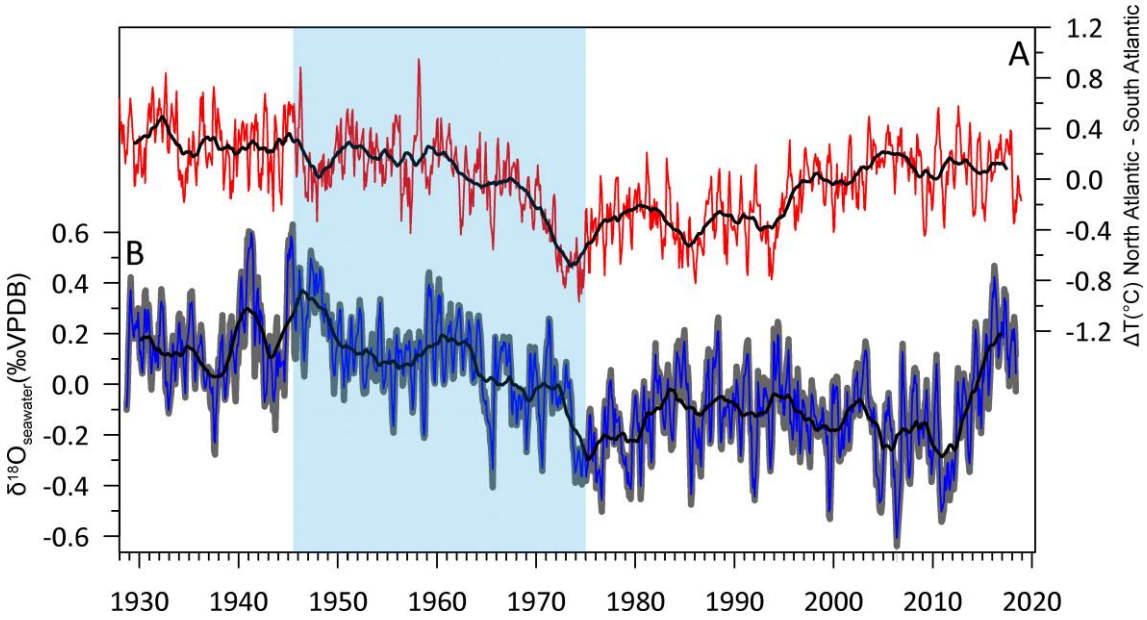

Figure 6. (A) Atlantic interhemispheric sea surface temperature (SST) difference from the HadISST product (Kennedy et al. 2019) (red line) calculated from area-integrated SST of the North Atlantic (Arctic Circle to equator) and the South Atlantic (Antarctic Circle to equator) between 68°W and 20°E. The black line is a 37-point running average. (B) Maracajaú reef seawater $\delta^{18}O$ reconstruction (blue line) according to equation (1) with γ_1 = −0.20‰/°C (Juillet-Leclerc and Schmidt 2001). Grey shadow is the error propagation according to equation 2 (separate errors are plotted for each data point), and the black line is a 37-point running average. A freshening trend (vertical blue shading) is evident from ca. 1945 to ca. 1975 and coincides with a decrease in the interhemispheric SST difference between North and South Atlantic (A).

Further evidence supporting a robust regional climate signal in our $\delta^{18}O_{seawater}$ reconstruction can be found in the comparison of our record with a recent SSS data compilation (Friedman et al. 2017). When comparing the two datasets for the time interval 1975 to 2018, which is a period of abundant instrumental SSS data, the Maracajaú reef *S. stellata* coral $\delta^{18}O_{seawater}$ reconstruction is confirmed to be a very good proxy for overall trends in regional SSS variability (Fig. 7). Statistical correlations can be assessed for two grid boxes included in Friedman et al. (2017); for grid-box 3, covering the area 5˚N-3˚S, 34˚W-45˚W r is 0.7 (p=0.006, N*=13, years 1975-2016), and for nearby grid-box 5, spanning 4˚N-5˚S, 20˚W-35˚W r=0.59 (p=0.03, N*=13, years 1975-2016). Before 1975, SSS observations are sparse, during some years observations are absent and values have

been interpolated over several years (Friedman et al., 2017, supplemental material). Hence, we do not consider SSS correlations to the coral-based $\delta^{18}O_{seawater}$ reconstruction prior to 1975 to be a valid exercise. Readers are further cautioned that direct calibration between the spatially averaged open-ocean SSS data and the single coastal observation from the coral $\delta^{18}O$ data is not appropriate because of the different amount of averaging inherent in each data source. However, the significant amount of shared variance between the datasets demonstrates that the $\delta^{18}O_{seawater}$ reconstruction based on the Maracajaú reef *S. stellata* coral, which extends back to 1928, provides a substantial improvement to existing regional SSS observation. In summary, the compelling similarity between the coral-based $\delta^{18}O_{seawater}$ reconstruction and the instrumental SSS data compilation for this region, during the time interval 1975 to 2015 (Friedman et al., 2017), strongly suggests that the coral proxy record captures large-scale hydrological signals in the surface ocean of the tropical western South Atlantic.

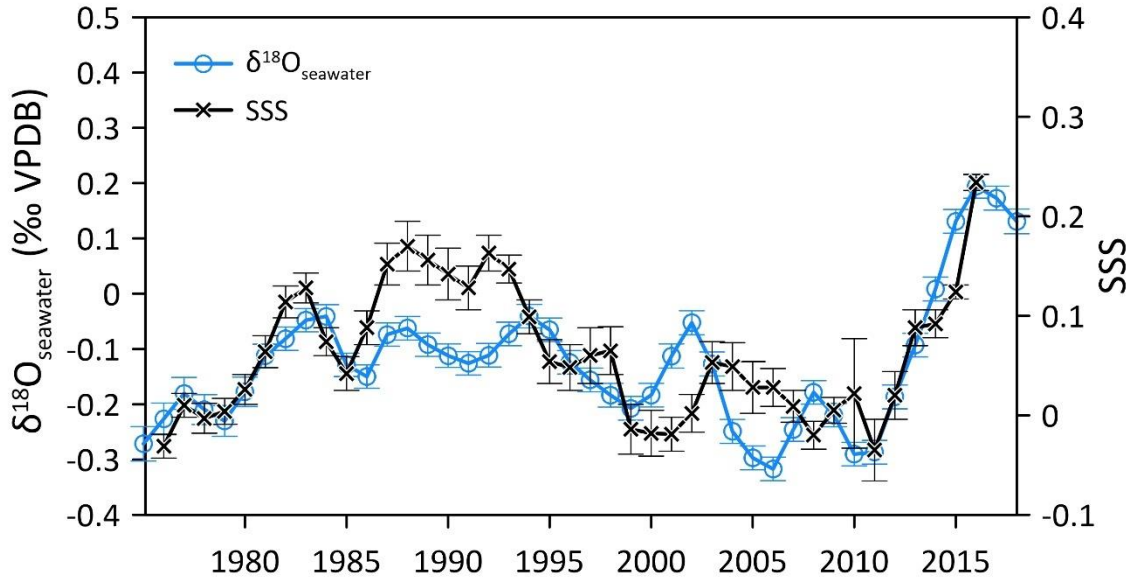

Figure 7. Instrumental sea surface salinity (SSS) data for the grid-box 5˚N-3˚S, 34˚W-45˚W (Friedman et al., 2017; crosses) and the Maracajaú reef *S. stellata* coral $\delta^{18}O_{seawater}$ reconstruction (circles) demonstrate the sensitivity of the coral $\delta^{18}O$ proxy to capture regional salinity variations. The gridded SSS data are freely available from the French Sea Surface Salinity Observation Service (www.legos.obs-mip.fr/observations/sss/). The salinity

data are available as annual March-February means that have been smoothed with a [121] binomial filter; the $\delta^{18}O_{seawater}$ data have been treated the same to enable comparison.

4.5. Role of the ITCZ in tropical Brazilian Atlantic Ocean change

By examining the $\delta^{18}O_{seawater}$ trend, we observed that most changes to the isotopic record occurred from 1945 to 1975, with a particularly steep decrease from the mid-1960s to the mid-1970s (Fig. 6C). The 1945–1975 drop represents a $\delta^{18}O_{seawater}$ change of −0.33‰ over a period of ca. 30 years. Using a $\delta^{18}O_{seawater}$–salinity relationship of −0.20 ± 0.03 ‰ per psu, as reported by Watanabe et al (2001, 2002) for seawater collected in the Caribbean Sea, the observed SSS freshening represents a decrease in SSS of ca. 1.65 psu.

The ITCZ position is seasonally regulated by the thermal equator, promoting its meridional migration throughout the tropics (Schneider et al. 2014). Long-term changes in the interhemispheric SST gradient would affect the latitudinal displacement of the ITCZ, shifting its position further north or south according to the SST gradient (Mulitza et al. 2017; Chiessi et al. 2021), affecting SSS in the western tropical South Atlantic and, more specifically, in the Maracajaú reef. A southward (northward) migration of the thermal equator would trigger a decrease (increase) in SSS at the Maracajaú reef.

The period from the mid-1940s to the mid-1970s was indeed marked by a decrease in the SST gradient between the North and the South Atlantic (Fig. 6B). This change is expected to have shifted the thermal equator to the south, resulting in a southward migration of the ITCZ and thus in increased precipitation over northern northeastern Brazil. Such an ITCZ migration is entirely consistent with the reconstructed $\delta^{18}O_{seawater}$ for the Maracajaú coral reef complex (Fig. 6C). We suggest that the decrease in $\delta^{18}O_{seawater}$ (and SSS) was produced by increased ITCZ-related precipitation over the Maracajaú reef, western tropical South Atlantic. Furthermore, this suggestion is consistent with a long-

438 term instrumental precipitation record for Caicó (6°27’35”S; 37°5’56”W), northeastern
439 Brazil, an inland location about 230 km from Maracajaú reef, which documents
440 increasing precipitation over the period of 1957 to 1972 (Fig. 6A) (Júnior and Lucena,
441 2020). Although the exact timing of the SSS freshening indicated by our Maracajaú reef
442 *S. stellata* coral derived $\delta^{18}O_{seawater}$ reconstruction does not perfectly match the increase
443 in continental precipitation for Caicó, the instrumental precipitation data clearly supports
444 the notion that a substantial input of freshwater into northern northeastern Brazil and the
445 western tropical South Atlantic occurred at least from the late 1950s to the early 1970s as
446 a result of changes in the interhemispheric Atlantic Ocean temperature gradient.

447 Although our results indicated a freshening in the western South Atlantic Ocean,
448 instrumental records assessed by Curry et al. (2003) indicated a salinity adjustment at the
449 Atlantic Ocean, with the tropics becoming more saline between ca. 1950 and 1990. At
450 the North Atlantic, the observation of Curry et al. (2003) was supported by Rosenheim et
451 al. (2005) which used sclerosponges records to reconstruct $\delta^{18}O_{seawater}$ of Salinity
452 Maximum Water from the North Atlantic for the period of 1890-1990, where they
453 observed a consistent increase in $\delta^{18}O_{seawater}$ from 1950 to 1990. Rosenheim et al (2005)
454 suggested that the change in salinity is related to recent intensification of the North
455 Atlantic Oscillation index, which is known to intensify the tradewinds in the tropical and
456 subtropical North Atlantic (Marshall et al. 2001). Stronger wind stress can consequently
457 increase evaporation. It might be easy to conclude that these studies are in contrast to the
458 freshening trend in our data, but they are focused on the broader tropics and subtropics,
459 not specifically the ITCZ-related SSS minimum region as in our study. An increasing
460 salinity trend over a broad swath of the tropics is consistent with increased evaporation
461 where E>P, but the water must go somewhere, and a concomitant decrease in salinity

within the ITCZ-related SSS minimum would indicate that at least some of it is transported to the deep tropics.

4.6. Connections to the Broader Climate System

The Maracajaú reef *S. stellata* coral derived $\delta^{18}O_{seawater}$ reconstruction is clearly related to regional SSS (Figure 7), with western tropical South Atlantic SSS linked to ITCZ-related precipitation (Tchilibou et al., 2015). The SSS changes reconstructed for the western tropical South Atlantic could represent either a migration of the ITCZ or a change in the strength of ITCZ-related precipitation, both potentially contributing to the observed $\delta^{18}O_{seawater}$ signal since 1928. The regional pattern of decreasing SSS in the western tropical South Atlantic over the last 90 years, with a strong decrease in the 1960s-1970s and a strong recovery in the 2010s, evidenced by our coral record, is consistent with the broader basin-wide pattern of climate variability over this period.

The strong 1960s-1970s SSS decrease shown by the Maracajaú reef *S. stellata* record is consistent with a southward ITCZ migration, in response to a sharp decrease in the Atlantic interhemispheric SST gradient (Fig. 6) (Thompson et al. 2010). The timing of the change coincides with the great salinity anomaly observed in the North Atlantic Subpolar Gyre (Friedman et al., 2017), and a decrease in Sahel rainfall (Hodson et al., 2014), that is inverse to the SSS freshening trend off northern northeastern Brazil, all these observations being consistent with a reduction in AMOC strength (Dima and Lohmann 2010, Zhang and Delworth 2005). Attempts to explore the causes of the 1960s-1970s interhemispheric temperature shift have ruled out volcanic, ENSO, and wintertime atmospheric advection forcings (Thompson et al., 2010). Modeling efforts indicate the change is likely unforced variability and may be related to changes in AMOC, although aerosol forcing cannot be completely discounted (Friedman 2020). Indeed, AMOC variability is well known to impact ITCZ location across different time scales (Schneider

et al. 2014; Mulitza et al. 2017; Liu et al. 2020), and if this cause is the major driver of the long-term trend in the Maracajaú reef *S. stellata* $\delta^{18}O_{seawater}$ reconstruction, then our new long-term record would be consistent with recent, though controversial, claims that the AMOC has slowed down over the 20th Century (Rahmstorf et al., 2015, Caesar et al., 2018, Thornalley et al., 2018, Caesar et al., 2021, Kilbourne et al., *in press*).

The length of the new Maracajaú reef *S. stellata* record also puts the well-recognized 1960s-1970s shift into a broader context, by showing a long-term decrease of $\delta^{18}O_{seawater}$ from 1928 to 2010, albeit punctuated by substantial interannual- to multidecadal-scale variations that culminate with an unprecedented trend to increased SSS from 2010–2018. This most recent trend and the large reconstructed $\delta^{18}O_{seawater}$ variations during the 1930s-1940s are not associated with a similar change in the interhemispheric temperature gradient (Fig. 6), unlike the 1960s–1970s shift. This observation highlights other processes besides the mean location of the ITCZ that can also influence regional SSS in the western tropical South Atlantic.

For instance, the intensity of the Hadley or the Walker Circulation could change the intensity of ITCZ-related rainfall. Servain et al. (2014) found evidence for intensification of the Hadley Circulation from 1960-2012. They found no significant trend in ITCZ location, as calculated by pseudo-windstress curl over those years, but instead documented warming temperatures centered under the ITCZ and intensification of the winds, consistent with an intensification of the Hadley cell. The Maracajaú reef *S. stellata* data are consistent with their study, showing no significant trend from 1960–2012 because the 1960s–1970s drop in SSS is balanced by the 2010s increase. Changes in the Walker circulation are thus likely to impact the Maracajaú reef $\delta^{18}O$ record. This is not surprising given the strong connection between Atlantic ITCZ-rainfall, especially during

March-April-May, and the Pacific Walker circulation (Saravanan and Chang 2000, Sasaki et al., 2015). The interaction between the Atlantic and Pacific can go both ways (McGregor et al., 2014), thus highlighting the potential for feedbacks between the tropical basins to be impacting the Maracajaú reef *S. stellata* records.

5. CONCLUSIONS

The first Brazilian *S. stellata* coral $\delta^{18}O_{seawater}$ reconstruction for the Maracajaú reef complex as presented herewith clearly shows that these corals are promising archives to understand key western tropical South Atlantic climate features, including changes in the ITCZ position and the related SSS variability. The new records of $\delta^{13}C$ and $\delta^{18}O$ values presented here are the longest reconstructions for the western tropical South Atlantic. The Maracajaú coral $\delta^{18}O$ values primarily records SST and the $\delta^{18}O$ of seawater, with no significant growth-related kinetic effects. $\Delta^{18}O_{seawater}$ was reconstructed by removing the SST contribution to the coral $\delta^{18}O$ record using a gridded instrumental SST product. The reconstructed $\delta^{18}O_{seawater}$ record is marked by a freshening trend from the 1940s to the 1970s, in agreement with a change in the interhemispheric temperature gradient during the same period, which also was coincident with the mid-20th Century hiatus in global warming.

Since ITCZ location is influenced by the interhemispheric temperature gradient, a decrease in the SST gradient between the North and the South Atlantic would have shifted the thermal equator to the south, resulting in southward migration of the ITCZ and increasing precipitation over northeastern Brazil. Such an ITCZ migration could be related to multidecadal- to centennial-scale variations in AMOC, although definitive reconstructions of AMOC history are required to test further this relationship. Besides changes in the latitudinal position of the ITCZ, some of the reconstructed $\delta^{18}O_{seawater}$ variability featured by our Maracajaú reef complex record, could also represent changes

in Hadley and/or Walker cell intensity, which would influence ITCZ-related precipitation and thus the western tropical South Atlantic SSS. A network of tropical South Atlantic coral-based SSS records, paired with similar records in the northern tropics, would facilitate distinguishing between intensity and latitudinal changes in the ITCZ, thus exploring in greater detail those processes that govern global heat distribution in the ocean–atmosphere system over decades to centuries, timescales that are difficult to interrogate with the short-duration instrumental data sets that are available.

In summary, the new Brazilian Maracajaú reef *S. stellata* geochemical records are an important step towards building a trans-hemispheric network and highlights the critical importance of tropical South Atlantic coral paleoclimate archives for improving our understanding of key global climate-system processes.

ACKNOWLEDGMENTS

The authors thank two anonymous reviewers as well as the editor for constructive comments that greatly improved this paper. This study was supported by Serrapilheira Institute (grant number Serra-1708-15845 to NSP). NSP, CMC, RKPK and GOL also thank the Brazilian National Council for Scientific and Technology Development (CNPq) for the research productivity scholarship (grants number 303372/2019-2 to NSP, 312458/2020-7 to CMC, 311449/2019-0 to RKPK and 310517/2019-2 to GOL). CMC acknowledges the financial support from FAPESP (grants 2018/15123-4, and 2019/24349-9), CAPES (grant 88881.313535/201901) and the Alexander von Humboldt Foundation. F.W.C and J.L. Campos were funded by FAPESP grant 2017/50085-3. KHK received support from the National Science Foundation grants OCE 1459636 and OCE 1829385, as well as NOAA Award NA20OAR4310481. This work represents UMCES contribution number XXXX. Determination of ^{230}Th ages was supported by grants from the Science Vanguard Research Program of the Ministry of Science and

Technology (MOST) (110-2123-M-002-009), the National Taiwan University (109L8926 to C.-C.S.), and the Higher Education Sprout Project of the Ministry of Education (110L901001 and 110L8907). NSP and RKPK are members of National Institute of Science and Technology for the Marine Tropical Environments (INCT AmbTropic grant CNPq 465634/2014-1).

REFERENCES

Al-Rousan S, Al-Moghrabi S, Pätzold J, Wefer G (2003) Stable oxygen isotopes in Porites corals monitor weekly temperature variations in the northern Gulf of Aqaba, Red Sea. Coral Reefs 22:346–356

Beck JW, Edwards RL, Ito E, Taylor FW, Recy J, Rougerie F, Joannot P, Henin C (1992) Sea-surface temperature from coral skeletal strontium/calcium ratios. Science 257:644–7

Brito SSB, Cunha APMA, Cunningham CC, Alvalá RC, Marengo JA, Carvalho MA (2018) Frequency, duration and severity of drought in the Semiarid Northeast Brazil region. Int J Climatol 38:517–529

Brocas WM, Felis T, Obert JC, Gierz P, Lohmann G, Scholz D, Kölling M, Scheffers SR (2016) Last interglacial temperature seasonality reconstructed from tropical Atlantic corals. Earth Planet Sci Lett 449:418–429

Cahyarini SY, Pfeiffer M, Timm O, Dullo WC, Schönberg DG (2008) Reconstructing seawater δ18O from paired coral δ18O and Sr/Ca ratios: Methods, error analysis and problems, with examples from Tahiti (French Polynesia) and Timor (Indonesia). Geochim Cosmochim Acta 72:2841–2853

Carilli JE, McGregor H V., Gaudry JJ, Donner SD, Gagan MK, Stevenson S, Wong H, Fink D (2014) Equatorial Pacific coral geochemical records show recent weakening of the Walker Circulation. Paleoceanography 29:1031–1045

Charles CD, Hunter D., Fairbanks RG (1997) REPORTS m a Interaction Between the ENSO and the Asian Monsoon in a Coral Record of Tropical Climate. Science (80-) 277:925–928

Cheng H, Edwards RL, Shen C-C, Polyak VJ, Asmerom Y, Woodhead J, Hellstrom J, Wang Y, Kong X, Spötl C, Wang X, Alexander EC (2013) Improvements in ^{230Th} dating, ^{230Th} and ^{234}U half-life values , and U–Th isotopic measurements by multi-collector inductively coupled plasma mass spectrometry. Earth Planet Sci Lett 371–372:82–91

Chiessi CM, Mulitza S, Taniguchi NK, Prange M, Campos MC, Häggi C, Schefuß E, Pinho TML, Frederichs T, Portilho-Ramos RC, Sousa SHM, Crivellari S, Cruz FW

(2021) Mid- to Late Holocene Contraction of the Intertropical Convergence Zone Over Northeastern South America. Paleoceanogr Paleoclimatology 36:e2020PA003936

Cobb KM, Westphal N, Sayani HR, Watson JT, Di Lorenzo E, Cheng H, Edwards RL, Charles CD (2013) Highly variable El Niño-Southern Oscillation throughout the Holocene. Science 339:67–70

Cohen AL, McConnaughey TA (2003) Geochemical Perspectives on Coral Mineralization.

Crivellari S, Viana PJ, Campos MDC, Kuhnert H, Machado Lopes AB, Cruz FW Da, Chiessi CM (2021) Development and characterization of a new in-house reference material for stable carbon and oxygen isotopes analyses. J Anal At Spectrom 36:1125–1134

Curry R, Dickson B, Yashayaev I (2003) A change in the freshwater balance of the Atlantic Ocean over the past four decades. Nature 426:826–829

DeLong KL, Maupin CR, Flannery JA, Quinn TM, Shen C-C (2016) Refining temperature reconstructions with the Atlantic coral Siderastrea siderea. Palaeogeogr Palaeoclimatol Palaeoecol

DeLong KL, Quinn TM, Taylor FW, Shen C-C, Lin K (2013) Improving coral-base paleoclimate reconstructions by replicating 350years of coral Sr/Ca variations. Palaeogeogr Palaeoclimatol Palaeoecol 373:6–24

Felis T (2020) Extending the instrumental record of ocean-atmosphere variability into the last interglacial using tropical corals. Oceanography 33:69–79

Huang B, Thorne PW, Banzon VF, Boyer T, Chepurin G, Lawrimore JH, Menne MJ, Smith TM, Vose RS, Zhang HM (2017) Extended reconstructed Sea surface temperature, Version 5 (ERSSTv5): Upgrades, validations, and intercomparisons. J Clim 30:8179–8205

Juillet-Leclerc A, Schmidt G (2001) A calibration of the oxygen isotope paleothermometer of coral aragonite from Porites. Geophys Res Lett 28:4135–4138

Kuffner IB, Roberts KE, Flannery JA, Morrison JM, Richey JN (2017) Fidelity of the Sr/Ca proxy in recording ocean temperature in the western Atlantic coral Siderastrea siderea. Geochemistry, Geophys Geosystems 18:178–188

Marshall J, Kushnir Y, Battisti D, Chang P, Czaja A, Dickson R, Hurrell J, McCartney M, Saravanan R, Visbeck M (2001) North Atlantic climate variability: Phenomena, impacts and mechanisms. Int J Climatol 21:1863–1898

Rayner NA, Parker DE, Horton EB, Folland CK, Alexander L V, Rowell DP, Kent EC, Kaplan A (2003) Global analyses of sea surface temperature, sea ice, and night marine air temperature since the late nineteenth century. J Geophys Res 108:4407

Reynolds RW, Rayner NA, Smith TM, Stokes DC, Wang W (2002) An improved in situ and satellite SST analysis for climate. J Clim 15:1609–1625

Rosenheim BE, Swart PK, Thorrold SR, Eisenhauer A, Willenz P (2005) Salinity change in the subtropical Atlantic: Secular increase and teleconnections to the

639 North Atlantic Oscillation. Geophys Res Lett 32:1–4

640 SWART PK (1983) Carbon and Oxygen Isotope Fractionation in Scleractinian Corals: a
641 Review. Earth-Science Rev 19:51–80

642 Swart PK, Grottoli a. (2003) Proxy indicators of climate in coral skeletons: a
643 perspective. Coral Reefs 22:313–315

644 Weber J, Woodhead P (1970) Carbon and oxygen isotope fractionation in the skeletal
645 carbonate of reef-building corals. Chem Geol 6:93–117

646 Evangelista H, Godiva D, Sifeddine A, Leão ZM a. N, Rigozo NR, Segal B, Ambrizzi
647 T, Kampel M, Kikuchi RKP, Le Cornec F (2007) Evidences linking ENSO and
648 coral growth in the Southwestern-South Atlantic. Clim Dyn 29:869–880

649 Evangelista H, Sifeddine A, Corrège T, Servain J, Dassié EP, Logato R, Cordeiro RC,
650 Shen C-C, Le Cornec F, Nogueira J, Segal B, Castagna A, Turcq B (2018)
651 Climatic Constraints on Growth Rate and Geochemistry (Sr/Ca and U/Ca) of the
652 Coral *Siderastrea stellata* in the Southwest Equatorial Atlantic (Rocas Atoll,
653 Brazil). Geochemistry, Geophys Geosystems 19:772–786

654 Evangelista H, Wainer I, Sifeddine A, Corrège T, Cordeiro RC, Lamounier S, Godiva
655 D, Shen C-C, Le Cornec F, Turcq B, Lazareth CE, Hu C-Y (2015) Southwestern
656 Tropical Atlantic coral growth response to atmospheric circulation changes
657 induced by ozone depletion in Antarctica. Biogeosciences Discuss 12:13193–
658 13213

659 Fairbanks RG, Dodge RE (1979) Annual periodicity of the the 18O/16O and 13C/12C
660 and ratios in the coral Montastrea annularis. Geochim Cosmochim Acta 43:1009–
661 1020

662 Fairbanks RG, Evans MN, Rubenstone JL, Mortlock RA, Broad K, Moore MD, Charles
663 CD (1997) Evaluating climate indices and their geochemical proxies found in
664 corals. Coral Reefs 16:S93–S100

665 Felis T (2020) Extending the instrumental record of ocean-atmosphere variability into
666 the last interglacial using tropical corals. Oceanography 33:69–79

667 Felis T, Pätzold J, Loya Y (2003) Mean oxygen-isotope signatures in Porites spp.
668 Corals: inter-colony variability and correction for extension-rate effects. Coral
669 Reefs 22:328–336

670 Felis T, Pätzold J, Loya Y, Fine M, Nawar AH, Wefer G (2000) A coral oxygen isotope
671 record from the northern Red Sea documenting NAO, ENSO, and North Pacific
672 teleconnections on Middle East climate variability since the year 1750.
673 Paleoceanography 15:679–694

674 Felis T, Rimbu N (2010) Mediterranean climate variability documented in oxygen
675 isotope records from northern Red Sea corals—A review. Glob Planet Change
676 71:232–241

677 Fowell SE, Sandford K, Stewart JA, Castillo KD, Ries JB, Foster GL (2016) Intra-reef
678 variations in Li/Mg and Sr/Ca sea surface temperature proxies in the Caribbean
679 reef-building coral *Siderastrea siderea*. Paleoceanography 1315–1329

680 Friedman AR, Reverdin G, Khodri M, Gastineau G (2017) A new record of Atlantic sea

surface salinity from 1896 to 2013 reveals the signatures of climate variability and long-term trends. Geophys Res Lett 44:1866–1876

Gagan MK, Ayliffe LK, Hopley D, Cali JA, Mortimer GE, Chappell J, Mcculloch MT, Head MJ (1998) Temperature and surface-ocean water balance of the mid-holocene tropical western pacific. Science 279:1014–8

Gagan MK, Chivas AR, Isdale PJ (1994) High-resolution isotopic records from corals using ocean temperature and mass-spawning chronometers. Earth Planet Sci Lett 121:549–558

Gagan MK, Chivas AR, Isdale PJ (1996) Timing coral-based climatic histories using 13C enrichments driven by synchronized spawning. Geology 24:1009–1012

Grottoli a. G, Wellington GM (1999) Effect of light and zooplankton on skeletal δ 13 C values in the eastern Pacific corals Pavona clavus and Pavona gigantea. Coral Reefs 18:29–41

Hathorne EC, Felis T, Suzuki A, Kawahata H, Cabioch G (2013) Lithium in the aragonite skeletons of massive Porites corals: A new tool to reconstruct tropical sea surface temperatures. Paleoceanography 28:

Hereid KA, Quinn TM, Taylor FW, Shen C-C, Lawrence Edwards R, Cheng H (2012) Coral record of reduced El Nino activity in the early 15^{th} to middle 17^{th} centuries. Geology 41:51–54

Hetzinger S, Pfeiffer M, Dullo W-C, Zinke J, Garbe-Schönberg D (2016) A change in coral extension rates and stable isotopes after El Niño-induced coral bleaching and regional stress events. Sci Rep 6:32879

Hiess J., Condon DJ., McLean N. and Noble SR. (2012) $^{238}U/^{235}U$ systematics in terrestrial uranium-bearing minerals. Science 355, 1610-1614.

Huang B, Thorne PW, Banzon VF, Boyer T, Chepurin G, Lawrimore JH, Menne MJ, Smith TM, Vose RS, Zhang HM (2017) Extended reconstructed Sea surface temperature, Version 5 (ERSSTv5): Upgrades, validations, and intercomparisons. J Clim 30:8179–8205

Jaffey AH, Flynn KF, Glendenin LE, Bentley WC and Essling AM. (1971) Precision measurement of half-lives and specific activities of ^{235}U and ^{238}U. Phys. Rev. C 4, 1889–1906.

Juillet-Leclerc A, Schmidt G (2001) A calibration of the oxygen isotope paleothermometer of coral aragonite from Porites. Geophys Res Lett 28:4135–4138

Júnior JBC, Lucena RL (2020) Analysis of Precipitation Using Mann-Kendall and Kruskal-Wallis Non-Parametric Tests. Mercator 19:1–14

Keeling CD (1979) The Suess effect: 13Carbon-14Carbon interrelations. Environ Int 2:229–300

Kennedy JJ, Rayner NA, Atkinson CP, Killick RE (2019) An Ensemble Data Set of Sea Surface Temperature Change From 1850: The Met Office Hadley Centre HadSST.4.0.0.0 Data Set. J Geophys Res Atmos 124:7719–7763

Kikuchi RKP, Oliveira MDM, Leão ZMAN (2013) Density banding pattern of the south

western Atlantic coral Mussismilia braziliensis. J Exp Mar Bio Ecol 449:207–214

Klein R, Tudhope AW, Chilcott CP, Pätzold J, Abdulkarim Z, Fine M, Fallick AE, Loya Y (1997) Evaluating southern Red Sea corals as a proxy record for the Asian monsoon. Earth Planet Sci Lett 148:381–394

Knutson TR, Zhang R, Horowitz LW (2016) Prospects for a prolonged slowdown in global warming in the early 21st century. Nat Commun 7:1–12

Kotov S, Pälike H (2018) QanalySeries – a cross-platform time series tuning and analysis tool.

Laborel J (1970) Les peuplements de madréporaires des cotes tropicales du Brésil. Ann L'Université D'Abidjan 2: 260

Leão ZMAN, Kikuchi RKP, Ferreira BP, Neves EG, Sovierzoski HH, Oliveira MDM, Maida M, Correia MD, Johnsson R (2016) Brazilian coral reefs in a period of global change: A synthesis. Brazilian J Oceanogr 64:97–116

Lee J, Boyle EA, Suci I, Pfeiffer M, Meltzner AJ, Suwargadi B (2014) Coral-based history of lead and lead isotopes of the surface Indian Ocean since the mid-20th century. Earth Planet Sci Lett 398:37–47

Lins-de-Barros M, Pires DO (2007) COMPARISON OF THE REPRODUCTIVE STATUS OF THE SCLERACTINIAN CORAL SIDERASTREA STELLATA THROUGHOUT A GRADIENT OF 20º OF LATITUDE. Brazilian J Oceanogr 55:67–69

Linsley BK, Rosenthal Y, Oppo DW (2010) Holocene evolution of the Indonesian throughflow and the western Pacific warm pool. Nat Geosci 3:578–583

Liu W, Fedorov A V., Xie SP, Hu S (2020) Climate impacts of a weakened Atlantic meridional overturning circulation in a warming climate. Sci Adv 6:eaaz4876

Maupin CR, Quinn TM, Halley RB (2008) Extracting a climate signal from the skeletal geochemistry of the Caribbean coral Siderastrea siderea. Geochemistry, Geophys Geosystems 9:n/a-n/a

Mayal EM, Sial AN, Ferreira VP, Fisner M, Pinheiro BR (2009) Thermal stress assessment using carbon and oxygen isotopes from Scleractinia , Rocas Atoll , northeastern Brazil. 51:166–188

McConnaughey T (1989) 13C and 180 isotopic disequilibrium in biological carbonates : I . Patterns. 53:151–162

Mulitza S, Chiessi CM, Schefuß E, Lippold J, Wichmann D, Antz B, Mackensen A, Paul A, Prange M, Rehfeld K, Werner M, Bickert T, Frank N, Kuhnert H, Lynch-Stieglitz J, Portilho-Ramos RC, Sawakuchi AO, Schulz M, Schwenk T, Tiedemann R, Vahlenkamp M, Zhang Y (2017) Synchronous and proportional deglacial changes in Atlantic meridional overturning and northeast Brazilian precipitation. Paleoceanography 32:622–633

Murty SA, Bernstein WN, Ossolinski JE, Davis RS, Goodkin NF, Hughen KA (2018) Spatial and Temporal Robustness of Sr/Ca-SST Calibrations in Red Sea Corals: Evidence for Influence of Mean Annual Temperature on Calibration Slopes. Paleoceanogr Paleoclimatology 33:443–456

765 Nobre P, Shukla J (1996) Variations of Sea Surface Temperature , Wind Stress , and
766 Rainfall over the Tropical Atlantic and South America. J Clim 9:

767 Omata T, Suzuki A, Kawahata H, Nojima S, Minoshima K, Hata A (2006) Oxygen and
768 carbon stable isotope systematics in Porites coral near its latitudinal limit: The
769 coral response to low-thermal temperature stress. Glob Planet Change 53:137–146

770 Pätzold J (1984) Growth rhythms recorded in stable isotopes and density bands in the
771 reef coral Porites lobata (Cebu, Philippines). Coral Reefs 3:87–90

772 Pereira NS, Sial AN, Frei R, Ullmann C V, Korte C, Kikuchi RKP, Ferreira VP,
773 Kilbourne KH (2017) The potential of the coral species Porites astreoides as a
774 paleoclimate archive for the Tropical South Atlantic Ocean. J South Am Earth Sci
775 77:276–285

776 Pereira NS, Sial AN, Kikuchi RKP, Ferreira VZP, Ullmann C V., Frei R, Cunha AMC
777 (2015) Coral-based climate records from tropical South Atlantic: 2009/2010 ENSO
778 event in C and O isotopes from Porites corals (Rocas Atoll, Brazil). An Acad Bras
779 Cienc 87:1939–1957

780 Pereira NS, Sial AN, Kilbourne KH, Liu SC, Shen CC, Ullmann C V., Frei R, Korte C,
781 Kikuchi RKP, Ferreira VP, Braga BLSS (2018) Carbon stable isotope record in the
782 coral species Siderastrea stellata: A link to the Suess Effect in the tropical South
783 Atlantic Ocean. Palaeogeogr Palaeoclimatol Palaeoecol 497:82–90

784 Pereira NS, Voegelin AR, Paulukat C, Sial AN, Ferreira VP (2016) Chromium-isotope
785 signatures in scleractinian corals from the Rocas Atoll , Tropical South Atlantic.
786 Geobiology 14:54–67

787 Pfeiffer M, Reuning L, Zinke J, Garbe-Schönberg D, Leupold M, Dullo W (2019) 20th
788 Century δ 18 O Seawater and Salinity Variations Reconstructed From Paired δ 18
789 O and Sr/Ca Measurements of a La Reunion Coral. Paleoceanogr Paleoclimatology
790 34:2183–2200

791 Revelle R, Suess HE (1957) Carbon Dioxide Exchange Between Atmosphere and
792 Ocean and the Question of an Increase of Atmospheric CO2 during the Past
793 Decades. Tellus 9:18–27

794 Reverdin G, Kestenare E, Frankignoul C, Delcroix T (2007) Surface salinity in the
795 Atlantic Ocean (30°S–50°N). Prog Oceanogr 73:311–340

796 Roos NC, Pennino MG, Carvalho AR, Longo GO (2019) Drivers of abundance and
797 biomass of Brazilian parrotfishes. Mar Ecol Prog Ser 623:117–130

798 Rosenheim BE, Swart PK, Thorrold SR, Eisenhauer A, Willenz P (2005) Salinity
799 change in the subtropical Atlantic: Secular increase and teleconnections to the
800 North Atlantic Oscillation. Geophys Res Lett 32:1–4

801 Santedicola, M.C.R., Kikuchi, R.K.P., Cunha, M.P., Domingues, R.M., Gonçalves,
802 P.M., 2008. Pilot study on Sr/Ca, Mg/Ca and Ba/Ca ratios in skeletons of
803 *Mussismilia braziliensis* (Verrill, 1868) as sea surface temperature (SST) proxy in
804 the coast of Bahia, Eastern Brazil, in: Oceanografia e Mudanças Globais. Instituto
805 Oceanográfico, São Paulo.

806 Santos, C.L.A., Vital, H., Amaro, V.E., Kikuchi, R.K.P., 2007. Mapping of the
807 submerged reefs in the coast of the Rio Grande do Norte, near Brazil: Macau to

808 Maracajau. Rev. Bras. Geofis. 25, 27–36.

809 Saenger C, Cohen AL, Oppo DW, Hubbard D (2008) Interpreting sea surface
810 temperature from strontium/calcium ratios in Montastrea corals: Link with growth
811 rate and implications for proxy reconstructions. Paleoceanography 23:

812 Schneider T, Bischoff T, Haug GH (2014) Migrations and dynamics of the intertropical
813 convergence zone. Nat 2014 5137516 513:45–53

814 Servain J, Caniaux G, Kouadio YK, McPhaden MJ, Araujo M (2014) Recent climatic
815 trends in the tropical Atlantic. Clim Dyn 43:3071–3089

816 Shen C-C, Wu C-C, Cheng H, Edwards R, Hsieh Y-T, Gallet S, Chang C-C, Li T-Y,
817 Lam D, Kano A, Hori M, Spöt C (2012) High-precision and high-resolution
818 carbonate ^{230}Th dating by MC-ICP-MS with SEM protocols. Geochim Cosmochim
819 Acta 99:71–86

820 Shen C-C, Li K-S, Sieh K, Natawidjaja D, Cheng H, Wang X, Edwards RL, Dinh DD,
821 Hsieh Y-T, Fan T-Y, Meltzner AJ, Taylor FW, Quinn TM, Chiang H-W,
822 Kilbourne KH (2008) Variation of initial 230 Th / 232 Th and limits of high
823 precision U–Th dating of shallow-water corals. 72:4201–4223

824 Silva ICBS, Liparini A, Pereira NS, Braga BLSS, Sial AN, Liu S, Shen C, Kikuchi RKP
825 (2019) Assessing the growth rate of the South Atlantic coral species Mussismilia
826 hispida (Verrill , 1902) using carbon and oxygen stable isotopes. J South Am
827 Earth Sci 96:1–9

828 Stefano C, Viana PJ, Campos MC, Kuhnert H, Lopes ABM, Cruz FW, Chiessi CM
829 (2021) Development and characterization of a new in-house reference material for
830 stable carbon and oxygen isotopes analyses. J Anal At Spectrom 36:1125–1134

831 Swart PK (1983) Carbon and Oxygen Isotope Fractionation in Scleractinian Corals: a
832 Review. Earth-Science Reviews 19:51–80

833 Swart PK, Greer L, Rosenheim BE, Moses CS, Waite AJ, Winter A., Dodge RE,
834 Helmle K (2010) The ^{13}C Suess effect in scleractinian corals mirror changes in the
835 anthropogenic CO_2 inventory of the surface oceans. Geophys Res Lett 37: L05604.

836 Swart PK, Grottoli a. (2003) Proxy indicators of climate in coral skeletons: a
837 perspective. Coral Reefs 22:313–315

838 Testa V, Bosence DWJ (1999) Physical and biological controls on the formation of
839 carbonate and siliciclastic bedforms on the north-east Brazilian shelf.
840 Sedimentology 46:279–301

841 von Reumont J, Hetzinger S, Garbe-Schönberg D, Manfrino C, Dullo C (2018)
842 Tracking Interannual- to Multidecadal-Scale Climate Variability in the Atlantic
843 Warm Pool Using Central Caribbean Coral Data. Paleoceanogr Paleoclimatology
844 33:395–411

845 Waliser DE, Gautier C (1993) A Satellite-derived Climatology of the ITCZ. J Clim
846 6:2162–2174

847 Watanabe, T., A. Winter, and T. Oba (2001) Seasonal changes in sea surface
848 temperature and salinity during the little Ice Age in the Caribbean Sea deduced
849 from Mg/Ca and ^{18}O/^{16}O ratios in corals, Mar. Geol., 173, 21– 35,

850 doi:10.1016/S0025-3227(00)00166-3.

851 Watanabe, T., A. Winter, T. Oba, R. Anzai, and H. Ishioroshi (2002) Evaluation of the
852 fidelity of isotope records as an environmental proxy in the coral Montastrea, Coral
853 Reefs, 21, 169–178.

854 Weber J, Woodhead P (1970) Carbon and oxygen isotope fractionation in the skeletal
855 carbonate of reef-building corals. Chemical Geology 6:93–117

856 Weerabaddana MM, DeLong KL, Wagner AJ, Loke DWY, Kilbourne KH, Slowey N,
857 Hu HM, Shen CC (2021) Insights from barium variability in a Siderastrea siderea
858 coral in the northwestern Gulf of Mexico. Marine Pollution Bulletin 173: 112930